Bioresource Technology 408 (2024) 131126

Contents lists available at ScienceDirect

Bioresource Technology

journal homepage: www.elsevier.com/locate/biortech

Conversion of wine lees and waste activated sludge into caproate and heptanoate: Thermodynamic and microbiological insights

A. Lanfranchi [a,b,*], E. Desmond-Le Quéméner [a], J.A. Magdalena [a,c], C. Cavinato [b], E. Trably [a]

[a] INRAE, Univ Montpellier, LBE, 102 Avenue Des Etangs, 11100 Narbonne, France
[b] Dipartimento di Scienze Ambientali, Informatica e Statistica, Università Ca' Foscari Venezia, Mestre 30174, Italy
[c] Vicerrectorado de Investigación Y Transferencia de La Universidad Complutense de Madrid, 28040 Madrid, Spain

HIGHLIGHTS

- A mixture of C6 and C7 was obtained by co-fermenting wine lees and WAS.
- Highest C6 and C7 selectivity of 40.2 % observed at 40 gCOD/L.
- Fast-growing chain-elongating microbiome led by *Clostridiaceae* and *Oscillospiraceae*.
- At 70 and 100 gCOD/L, ethanol-based chain elongation shifted to a lactate-based one.
- pH_2 is a fundamental parameter to control EEO and increase C6 and C7 selectivity.

GRAPHICAL ABSTRACT

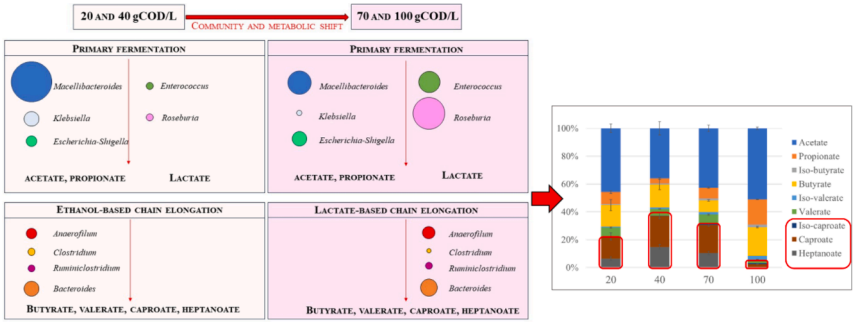

ARTICLE INFO

Keywords:
Chain elongation
Ethanol oxidation
Thermodynamics
Winery waste
Microbial community

ABSTRACT

In this study, wine lees and waste activated sludge (WAS) were co-fermented for the first time in a 4:1 ratio (COD basis) at 20, 40, 70 and 100 gCOD/L, in batch at 37 °C and pH 7.0. The substrates were successfully converted to caproate (C6) and heptanoate (C7) with a high selectivity (40.2 % at 40 gCOD/L). The rapidly-growing chain-elongating microbiome was enriched in *Clostridiaceae* and *Oscillospiraceae*, representing together 3.4–8.8 % of the community. Substrate concentrations higher than 40 gCOD/L negatively affected C6 and C7 selectivities and yields, probably due to microbial inhibition by high ethanol concentrations (15.82–22.93 g/L). At 70 and 100 gCOD/L, chain elongation shifted from ethanol-based to lactate-based, with a microbiome enriched in the lactic acid bacteria *Roseburia intestinalis* (27.3 %) and *Enterococcus hirae* (13.8 %). The partial pressure of H_2 (pH_2) was identified by thermodynamic analysis as a fundamental parameter for controlling ethanol oxidation and improving C6 and C7 selectivities.

1. Introduction

Upgrading biodegradable waste streams into fuels and chemicals is a crucial step in achieving full circular economy by effectively closing the carbon cycle. For this reason, residues valorization has become a core aspect of the EU Green Deal, a growth strategy aiming at developing a European circular bio-economy (European Commission, 2019). According to the EU Biorefinery Outlook, around 30–50 % of the European

* Corresponding author at: INRAE, Univ Montpellier, LBE, 102 Avenue des Etangs, 11100 Narbonne, France.
E-mail address: alanfra@outlook.it (A. Lanfranchi).

https://doi.org/10.1016/j.biortech.2024.131126
Received 7 May 2024; Received in revised form 27 June 2024; Accepted 16 July 2024
Available online 17 July 2024

high-value-added organic chemicals will be produced from organic waste by 2030 (Platt et al., 2021). However, converting complex waste into platform molecules with competitive yields and selectivities is still a challenging task.

Medium-chain carboxylic acids (MCCAs), i.e., carboxylates with six to ten carbon atoms, are chemical building blocks having wide industrial applications, explaining the increasing market demand. At present, MCCAs are mainly obtained as a by-product of palm kernel oil refining (Shahid, 2005). Palm kernel oil is relatively rich in caprylate (C8, ~55 %) and caprate (C10, ~ 42 %), but the C6 concentration is limited to only ~2 % w/w (Turpeinen and Merimaa, 2011). Such low C6 content limits the production to 25 ktons/year with a high selling price of 1.88–2.09 €/kg (Moscoviz et al., 2018). In addition, C7 is mostly derived from castor oil through the oxidation of heptaldehyde, with a maximum selectivity of 25 % w/w (Das et al., 1989; Springer and Lappe, 2001). Current research efforts are focusing on increasing these low yields and selectivities in C6 and C7 *via* sustainable microbial routes, the so-called chain elongation process. Chain elongation is a secondary anaerobic fermentation process occurring *via* the reverse β-oxidation pathway (RBO). RBO pathway consists of increasing the length of the carboxylic acid chain through sequential additions of two atoms of carbon using ethanol or lactate as preferred electron donors. These reactions are thermodynamically feasible under standard conditions corrected for pH = 7 as indicated by Gibbs energy changes denoted ΔG°' (Eq.1) (Roghair et al., 2018).

$$RBO: 5C_xH_{2x-1}O_2^- + 6C_2H_6O \rightarrow 5C_{x+2}H_{2x+3}O_2^- + C_2H_3O_2^- + 4H_2O + H^+ + 2H_2$$

$$\Delta G^{0'} = -184.3\frac{kJ}{mol}(C4\rightarrow C6)$$

$$\Delta G^{0'} = -188.3\frac{kJ}{mol}(C5\rightarrow C7) \quad (1)$$

However, the competitiveness of this biological process is hampered by the high cost and environmental impact of sugar-based feedstocks and ethanol (Chen et al., 2017; Debergh and Van Dael, 2022). While the use of waste streams such as wine lees can represent an environmentally and economically sustainable feedstock, providing ethanol as electron donor for the RBO pathway, steering fermentation pathways towards the desired end-products is challenging when using open-mixed cultures due to outcompeting microbial routes.

The major metabolic pathway outcompeting ethanol-based chain elongation is excessive ethanol oxidation (EEO), where ethanol is directly oxidized to acetate (Eq.2) at low partial pressure of H_2 (pH_2 = 0.0003–0.002 bar) (Roghair et al., 2018). This pathway is particularly detrimental to RBO process when costly external ethanol is supplied to the system. Nonetheless, partial EEO can play a positive role in upgrading ethanol-rich waste streams such as wine lees by transforming part of the ethanol in acetate, which could be further elongated to butyrate (C4) and caproate (C6).

$$EEO = C_2H_6O + H_2O \rightarrow C_2H_3O_2^- + H^+ + 2H_2$$

$$\Delta G^{0'} = 9.6\,\mathrm{kJ/mol} \quad (2)$$

EEO is often close to thermodynamic equilibrium, as illustrated by the value of ΔG°' close to zero (Eq.2). Thermodynamic state analysis can therefore be a useful tool for process understanding and control, since the thermodynamic feasibility of EEO can be determined under specific experimental conditions and, in turn, the experimental conditions can be tuned to boost the desired reactions (Kleerebezem and Van Loosdrecht, 2010).

With this type of fermentation and process control, the high ethanol concentrations (87–107 g/L) contained in wine lees (Kucek et al., 2016b) are foreseen as a valuable resource to upgrade the concentration in C6 and C7 through RBO and EEO in an open-mixed culture reactor. Meanwhile, the use of wine lees as substrate requires dilution to avoid fermentation inhibition due to ethanol toxicity. Dilution can be performed by co-fermentation with other organic waste such as waste activated sludge (WAS), simultaneously treating two types of waste generated by the winemaking process and reducing resource needs.

In light of this, the novelty of this study is to investigate systematically the effect of increasing substrate concentrations on the anaerobic co-fermentation of wine lees and WAS for the production of C6 and C7. These two wastes from the winemaking process have not been previously combined in anaerobic fermentation and could benefit the process sustainability in the perspective of scale-up. A thermodynamic analysis and mass balance of the system were performed to better understand key metabolic pathways and identify the best operational conditions for better control over the RBO process. The microbial community was also analyzed to identify the key microbial species catalyzing the observed reactions.

2. Materials and methods

2.1. Substrates characterization

This study used red wine lees from the INRAE research unit of Pech Rouge (France) and WAS was collected at the wastewater treatment plant of Narbonne (France). These substrates were characterized before being stored at −20 °C. Red wine lees had a soluble COD content of 228.17 ± 5.04 gCOD/L, 98.0 % of which was ethanol (107.3 g/L), and a total COD content of 353.33 ± 6.62 gCOD/L. The biodegradable COD (bCOD) corresponded to 80.3 % of the total COD. WAS underwent centrifugation and the liquid and solid fractions were stored separately at −20 °C, to reproduce a thickened WAS with 40 gTS/L for the experiments. The WAS had a VS/TS ratio of 0.78 and a total COD content of 50.19 ± 0.27 gCOD/L, corresponding to a bCOD of 35.8 %.

2.2. Anaerobic co-fermentation experiments

Anaerobic co-fermentation was performed on wine lees and WAS with a 4:1 ratio on a total COD basis, which was representative of waste fluxes of a winemaking company situated in Northern Italy (Da Ros et al., 2017). Batch experiments were conducted in quadruplicate, in 1L glass bottles with a working volume of 0.5 L and equipped with custom necks for sampling. Fermentation was performed by the indigenous microbial community of the substrates, without inoculum addition. The pH was initially adjusted at 7 by adding 8 M NaOH, and the medium was buffered with 400 mM HEPES (2-[4-(2-Hydroxyethyl)piperazin-1-yl] ethane-1-sulfonic acid). Before incubation at 37 °C, the headspace was flushed with N_2 for 5 min to ensure anaerobic conditions. Bottles were mechanically stirred before sampling. Increasing substrates concentrations of 20, 40, 70 and 100 gCOD/L were tested, which corresponded to initial ethanol concentrations (g/L) of 4.55 ± 0.11, 9.20 ± 0.17, 15.82 ± 0.20, and 22.93 ± 0.29, respectively. To reach the target concentrations, substrates were diluted with tap water. The tests were closed when methane production started. Bottles were sampled daily (10 mL) for metabolites, pH, and microbial community analyses. Online monitoring of gas production and composition was performed every 2 h.

2.3. Analytical methods

Total and soluble COD of the substrates was measured with commercial kits (Lovibond, Germany). bCOD was determined by near-infrared spectroscopy (Lesteur et al., 2011). pH was daily monitored with a Five Easy™ pHmeter (Mettler Toledo). Carboxylates concentrations were determined by gas-chromatography (GC) and ethanol, lactate, glycerol and 1,3-propanediol (1,3-PDO) were monitored by High-Performance Liquid Chromatography as described elsewhere (Noguer et al., 2022). Biogas production and composition were

monitored with a micro-gas chromatograph (MicroGC, SRA l-GC R3000) (Noguer et al., 2022).

2.4. Calculations

The yield indicates the amount of bCOD of the substrates converted into fermentative metabolites. For the liquid products (carboxylates and 1,3-propanediol), yield was calculated as it follows (Eq. (3):

$$Yield\ \frac{g\,CODprod}{g\,bCOD} = \frac{Products\ concentration\left(\frac{g\ COD}{L}\right) \times working\ volume\ (L)}{Substrates'\ concentration\left(\frac{g\ bCOD}{kg}\right) \times substrates\ inserted\ (kg)} \quad (3)$$

where working volume was the real working volume, considering samples withdrawal.

For the gaseous products, yield was calculated as mL gas/g bCOD inserted. The volume of gas produced was calculated through the pressure variations, as detailed in Roslan et al. (2023). Carboxylates selectivity was expressed as a percentage on a COD basis of the total carboxylates produced.

2.5. Microbial community analysis

Microbiological analysis was performed by 16S rRNA gene Illumina sequencing on the biomass pellet resulting from sample centrifugation according to Noguer et al. (2022). For each condition, the samples at day 4 were selected because it corresponded to the end of the test at a substrate concentration of 20, 40, and 70 gCOD/L. For the condition at 100 gCOD/L, the sample at day 7 was also analyzed. Sequences were submitted to GenBank, under the accession number PRJNA1028514. The rRNA sequences of OTUs with relative abundance ≥ 1 % were then used for Megablast to search within the NCBI nucleotide database.

Bioinformatic analyses were conducted in R version 4.3.0 with the packages *phyloseq*, *microbiome*, *vegan*, *MicEco, microeco*. Graphs were realized with *ggplot2*. Spearman's correlation between the environmental variables and the OTUs was calculated with the *trans$env* function in the *microeco* package. To evaluate the distance between samples, Principal Coordinates Analysis (PCoA) was performed with the *capscale* function in the *vegan* package. The correlation between microbiome composition and environmental factors was investigated by fitting the PCoA scores with the *envfit vegan* function.

2.6. Thermodynamic analysis and mass balance

Thermodynamic calculations were performed as indicated by Kleerebezem and Van Loosdrecht (2010), using their ΔG_f^0 and H_f^0 values. The missing H_f^0 values were retrieved from the OBGIT thermodynamic database in the R package *CHNOSZ*. The standard variation in Gibbs free energy ($\Delta G^{0'}$), reported also in Eq. (1) and (2), was calculated at T = 25 °C, pH = 7, and all aqueous and gaseous species at 1 atm. Temperature corrections to 37 °C to $\Delta G^{0'}$were made by applying the Gibbs-Helmholtz equation. For each condition, the variation in Gibbs free energy of reaction (ΔG) was daily determined for the lactate-based and ethanol-based chain elongation of acetate to butyrate (C2→C4), butyrate to caproate (C4→C6), propionate to valerate (C3→C5), valerate to heptanoate (C5→C7) and for the EEO. At day 0, H_2 partial pressure was calculated from the equation of decomposition of water in O_2 and H_2 at equilibrium, resulting in $pH_2 = 4.07*10^{-38}$ bar. For chain elongation, at day 0 the concentrations of butyrate, caproate, valerate and heptanoate were estimated as threshold values of detectability of the GC (0.01 g/L).

Once the feasibility of chain elongation and EEO was determined, biomass production was calculated considering it to occur from acetate in ethanol-based chain elongation and EEO, and from lactate in lactate-based chain elongation. The stoichiometry of biomass growth was estimated with Heijnen's Gibbs energy dissipation method (Kleerebezem and Van Loosdrecht, 2010). Mass balance was performed to understand the metabolic pathways involved in chain elongation and acetate production.

2.7. Statistical analyses

A Kruskal-Wallis statistical test was performed to evaluate the significance of the differences observed between all the conditions tested. The Mann-Whitney-Wilcoxon statistical test was applied to compare two specific conditions. The level of significance was set at $p < 0.05$. Statistical analyses were conducted in R version 4.3.0 with the *stats* package.

3. Results and discussion

3.1. Production of carboxylates: dynamics, selectivities, and yields

Carboxylates production and ethanol consumption started on day 1 at all substrate concentrations (Fig. 1). In all cases, the decrease of ethanol concentrations (from 9.47, 19.17, 32.98, and 47.78 to 3.01, 6.31, 23.13, and 38.30 gCOD/L) was accompanied by an increase in acetate concentrations (from 0.03 to 0.06 to 3.73, 5.93, 7.48, and 10.19 gCOD/L) at substrate concentrations of 20, 40, 70 and 100 gCOD/L, respectively. From day 3 to day 4, the decrease of ethanol concentrations accelerated at 20 and 40 gCOD/L, coinciding with an increase in MCCAs concentrations. This suggests that ethanol was consumed by chain elongation reactions to produce MCCAs from short-chain fatty acids (SCFAs). Interestingly, at high substrate concentrations (70 and 100 gCOD/L), ethanol consumption stopped from day 3 despite the occurrence of chain elongation, suggesting that some alternative electron donor was used, such as lactate or amino acids hydrolyzed from WAS or the yeast cells in wine lees (Fig. 1) (Bevilacqua et al., 2022). The role of amino acids as electron donors started being elucidated only recently (Bevilacqua et al., 2022; Wallace et al., 2004, 2003; Wu et al., 2023). Lactate is extensively reported as the main electron donor in chain elongation alongside ethanol, and the hypothesis that lactate was the other main electron donor was further supported by the microbial community composition, where lactate-producers increased their relative abundance at 70 and 100 gCOD/L (section 3.4) (Liu et al., 2024 and references therein). Overall, the fermentation process always resulted in ethanol removal within a range of 25.8–68.2 % (Table 1). Initial substrate concentration influenced the MCCAs production dynamics: at 20, 40 and 70 gCOD/L, MCCAs concentrations significantly increased at day 4. At 100 gCOD/L, this increase was slightly delayed and occurred at day 7.

In this study, chain elongation occurred from day 3, earlier than what was observed on similar substrates in batch conditions. In fact, San-Valero et al. (2019) reported that chain elongation started on day 5–6 on ethanol, acetate and/or butyrate at pH 6.8. At pH 7, with grape pomace inoculated with digestate from the anaerobic digestion of the organic fraction of municipal solid waste and acclimated to the anaerobic digestion of the same substrate, C6 production started on day 6

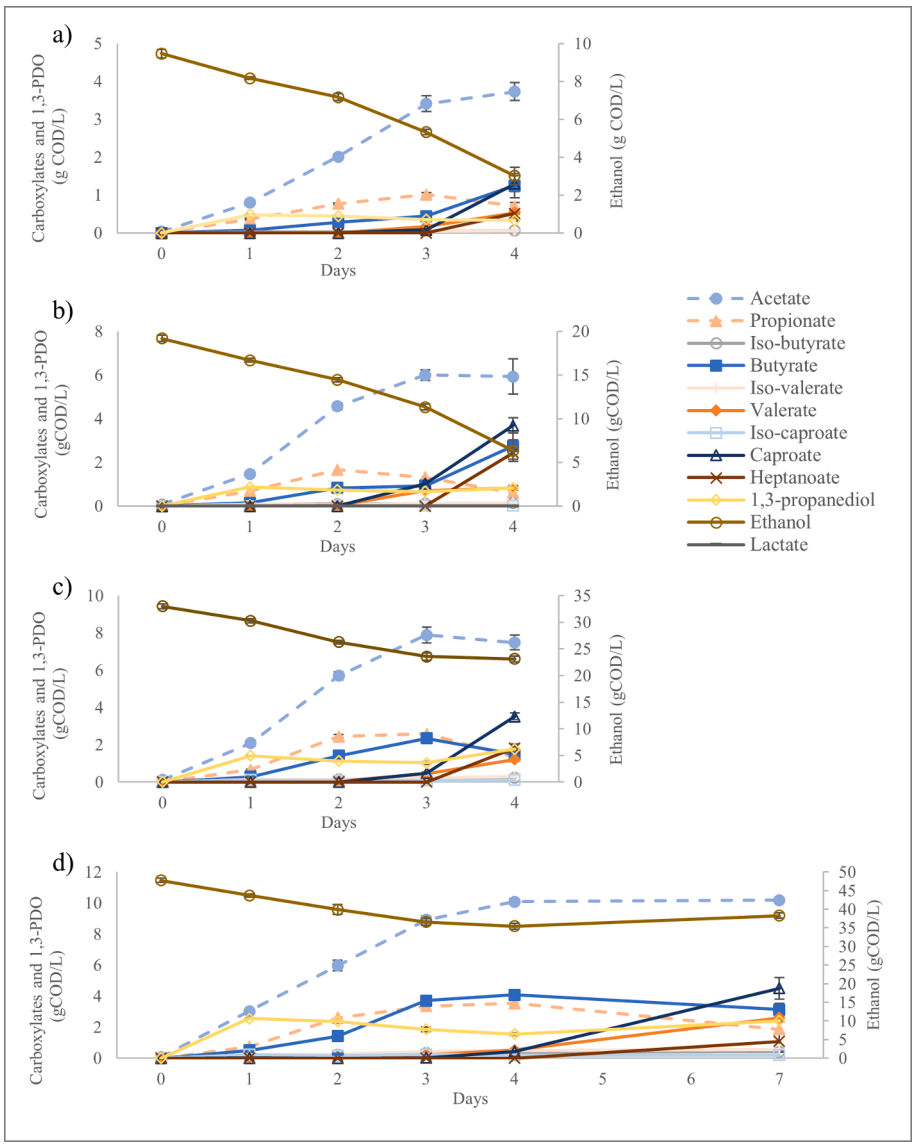

Fig. 1. Trend of the concentrations of carboxylates, 1,3-PDO, and ethanol at a substrate concentration (gCOD/L) of a) 20; b) 40; c) 70 and d) 100. The carboxylates considered as precursors of longer-chain carboxylates, i.e., acetate and propionate, were represented with dotted lines. For the main compounds (butyrate, valerate, caproate, and heptanoate), the longer the molecule, the darker the colour assigned to it.

(Martinez et al., 2022). This is attributable to the high food to microorganisms ratio (F/M) of 55.6 TVS/TVS applied in the latter study (calculated), requiring longer time for biomass growth and adaptation. In our experiment, WAS was a biologically active co-substrate and could be considered as microbial inoculum with an F/M of 4 TVS/TVS. Therefore, the lower F/M of 4 TVS/TVS applied in this experiment could explain the faster C6 production dynamics observed. In contrast, when inoculating winery wastewater with digested sludge issued from a wastewater treatment plant, no C6 was detected after 10 days, even at a low F/M of 1 (Esteban-Gutiérrez et al., 2018). This might have occurred due to the low pH applied (5.5), which was reported to reduce growth rates by 40 % in *C. kluyveri* pure cultures (Weimer and Stevenson, 2012). A comparable speed in the occurrence of chain elongation was reported only in Kim et al. (2021), where in 7 days anaerobic digestion sludge from a WAS anaerobic digestion system almost completely depleted 100 mM of lactate in presence of butyrate as the only co-substrate, generating caproate with a 56.3 % selectivity. The applied lactate concentration of 100 mM was similar to the ethanol concentration of 98.7 mM used in this study at 20 gCOD/L, where after 4 days 68 % of the ethanol was removed, generating MCCAs with a 22.9 % selectivity (Table 1). After 5 cycles of acclimation (i.e., 84 h), the microbiome was able to consume 100 mM of lactate and 20 mM of butyrate in 21 h, with a 73.5 % caproate selectivity (Kim et al., 2021). These results pave the way for future work on the substrates tested in this study, where the rate of chain elongation could be further improved and then confirmed in continuous reactors.

In this study C6 production began after 3 days, without a specific butyrate concentration threshold (day 2: 0.16, 0.45, 0.78, and 0.79 g/L of butyrate at a substrate concentration of 20, 40, 70, and 100 gCOD/L, respectively), in agreement with the study of San-Valero et al. (2019) on C6 production from pure cultures of *C. kluyveri*, where acetate and butyrate were simultaneously consumed for biomass growth from day 4.75, and the chain elongation process was carried out in parallel. Interestingly, some authors attributed the delay in C6 production to physiological reasons, after observing that it started only when a certain butyrate threshold was reached (2.5 and 0.45 g/L, after six and thirty-six days, respectively) (Martinez et al., 2022; Steinbusch et al., 2011).

Therefore, our results suggest a rapid adaptation of the microbial community, attributable to the fact that i) the microbiome of wine lees is already adapted to high ethanol concentrations; ii) wine lees contain

Table 1
Carboxylates percentages, products concentrations and yields, initial and final ethanol concentration, and ethanol removal at day 4 for all the tested conditions. "IC6 + C6 + C7" indicates the sum of *iso*-caproate, caproate and heptanoate.

Parameter	Unit	20	40	70	100
				gCOD/L	
Acetate	% (COD basis)	47.2 ± 3.1	38.9 ± 5.2	45.1 ± 2.4	51.1 ± 1.0
Propionate		9.0 ± 1.1	4.0 ± 0.4	8.2 ± 0.5	17.9 ± 0.2
Iso-butyrate		0.8 ± 0.1	0.8 ± 0.0	1.4 ± 0.1	2.1 ± 0.1
Butyrate		15.9 ± 4.1	18.0 ± 4.0	8.9 ± 0.5	20.7 ± 0.5
Iso-valerate		0.8 ± 0.0	1.0 ± 0.0	1.8 ± 0.1	2.5 ± 0.1
Valerate		6.7 ± 0.4	5.4 ± 0.2	7.3 ± 0.4	2.6 ± 0.2
Iso-caproate		0.0 ± 0.0	0.1 ± 0.1	0.6 ± 0.0	0.9 ± 0.0
Caproate		**16.5 ± 2.6**	**24.2 ± 2.2**	**21.2 ± 1.1**	**2.2 ± 0.3**
Heptanoate		**6.5 ± 1.4**	**16.0 ± 2.0**	**11.0 ± 1.3**	**0.0 ± 0.0**
MCCAs (IC6 + C6 + C7)		**22.9 ± 4.0**	**40.2 ± 4.3**	**32.9 ± 2.4**	**3.2 ± 0.3**
Acetate	gCOD/L	3.73 ± 0.25	5.94 ± 0.80	7.48 ± 0.41	10.08 ± 0.19
Propionate		0.71 ± 0.09	0.60 ± 0.06	1.36 ± 0.09	3.54 ± 0.03
Iso-butyrate		0.05 ± 0.00	0.13 ± 0.00	0.24 ± 0.02	0.40 ± 0.02
Butyrate		1.25 ± 0.33	2.74 ± 0.62	1.49 ± 0.09	4.09 ± 0.09
Iso-valerate		0.06 ± 0.00	0.14 ± 0.00	0.31 ± 0.02	0.49 ± 0.02
Valerate		0.53 ± 0.04	0.81 ± 0.04	1.20 ± 0.06	0.51 ± 0.04
Iso-caproate		0.00 ± 0.00	0.00 ± 0.02	0.11 ± 0.00	0.20 ± 0.00
Caproate		1.30 ± 0.20	3.68 ± 0.35	3.53 ± 0.18	0.44 ± 0.07
Heptanoate		0.51 ± 0.12	2.43 ± 0.30	1.83 ± 0.23	0.00 ± 0.00
TOT carboxylates		8.16 ± 0.40	16.48 ± 0.55	17.54 ± 0.81	19.75 ± 0.26
1,3-PDO		0.32 ± 0.02	0.82 ± 0.10	1.76 ± 0.05	1.56 ± 0.09
Yield	**g CODprod/g bCODin**	**0.52 ± 0.04**	**0.50 ± 0.04**	**0.33 ± 0.02**	**0.27 ± 0.00**
Initial ethanol concentration		**4.55 ± 0.11**	**9.20 ± 0.17**	**15.82 ± 0.20**	**22.93 ± 0.29**
Final ethanol concentration	**g/L**	1.45 ± 0.22	3.03 ± 0.59	11.10 ± 0.27	17.00 ± 0.34
Ethanol removal	**%**	**68.2 ± 5.1**	**67.1 ± 5.9**	**29.8 ± 2.4**	**25.8 ± 1.3**

yeasts and therefore nutrients (microelements, B vitamins) required for several wild-type chain-elongating microorganisms (Barker, 1947); iii) the simultaneous presence of acetate and butyrate in the fermentation broth had a synergistic effect on the growth rate and biomass concentration of *C. kluyveri*, which could also occur in other chain-elongating species (San-Valero et al., 2019).

Similarly to the dynamics, the MCCAs selectivity was highly influenced by the substrate concentration. As shown in Table 1, on day 4 it was 22.9 %, 40.2 %, 32.9 %, and 3.2 % (COD basis) at 20, 40, 70 and 100 gCOD/L, respectively. The selectivity at 100 gCOD/L increased on day 7, reaching 24.1 % with 18.8 % of C6. The highest value of 40.2 % was obtained at 40 gCOD/L, which was higher than at 70 gCOD/L (32.9 %, p-value = 0.02857).

Overall, a high MCCAs selectivity (22.9–40.2 %) was obtained for a short-term experiment. In batch, a comparable C6 selectivity of ~26 % (COD basis) was obtained after 31 days at pH 7.0 and 35 °C on winery wastewater, diluted to reach an initial ethanol concentration of 23 g/L of ethanol and 5 g/L of acetate. Interestingly, at the same temperature and pH 6.0, the highest C6 and C8 selectivities of 57.6 and 31.0 % were reached, while C7 (up to ~40 %) was produced mainly at acidic pH of 5.0–6.0 (Villegas-Rodríguez et al., 2024). C8 production was due to the use of ruminal inoculum, while the red wine endogenous microbiome had a higher C6 selectivity (Villegas-Rodríguez and Buitrón, 2021). These findings underline the pivotal role of microbiome and pH in MCCAs production and pave the way for improving selectivities on the co-fermentation of wine lees and WAS. On other complex substrates, higher selectivities were only reached in longer experiments carried out on grape pomace, office paper, and chicken and swine manures after 13, 27 and 76 days respectively, with values of ~77.0 % (calculated), ~51.0 % (calculated) and 58.8 %, respectively (Lonkar et al., 2016; Martinez et al., 2022; Zhang et al., 2020). In continuous, wine lees gave the highest MCCAs yield of 0.67 $gCOD_{carboxylates}/gCOD_{in}$ and a selectivity of 36 % for each C8 and C6 at an organic loading rate (OLR) of 5.8 gCOD/L·d at pH 5.2 (Kucek et al., 2016b). The higher C6 selectivity reported (36 % on COD basis) respect to the one observed in this study (24.2 % at 40 gCOD/L) is attributable to the different reactor configuration, and particularly to the continuous extraction of the MCCAs produced *via* an in-line membrane-based pertraction system. In fact, MCCAs removal kept C6 concentrations under the inhibitory threshold of 6.9–7.5 mM (1.77–1.93 gCOD/L) of undissociated acid (Ge et al., 2015), and the simultaneous broth recycling allowed further chain elongation of C6 to C8 with a final 36 % selectivity. Similarly, higher C6 selectivities of 32 % and 35 % were obtained in continuous processes with in-line product extraction (Agler et al., 2014; Carvajal-Arroyo et al., 2021).

The highest MCCAs selectivity of 40.2 % observed at 40 gCOD/L was mainly due to C7 (16.0 %), that was higher than at 70 gCOD/L (11.0 %) (p-value = 0.02857). In fact, the percentage of C6 (24.2 %) was similar to that obtained at 70 gCOD/L (21.2 %) (p-value = 0.1714). This is attributable to a better substrate conversion to valerate, that reached the highest yield of 0.023 $gCOD_{carboxylates}/g\ bCOD_{in}$ on day 3 (Supplementary Material) and was then elongated to C7. The C7 selectivity obtained herein (16 % in COD basis) is the highest observed at pH 7.0 on complex substrates without external ethanol supplementation. With ethanol addition, Zhang et al. (2020b) reached the highest C7 selectivity (36.4 %) in the batch two-stage fermentation of swine manure, with a final C7 concentration of 6.4 gCOD/L after 55 days of chain elongation phase and 76 days of total fermentation. As mentioned before, Villegas-Rodríguez et al. (2024) reached a 40 % C7 selectivity on winery wastewater at 30 °C and pH 5.0, while no C7 was detected at pH 7.0 and 35 °C. However, the different length of these experiments did not allow for a direct comparison with our short-term fermentation.

All conditions assessed resulted in a lower C7 selectivity compared to C6. This was expected in the upgrading of ethanol-rich wastes, since the main SCFA produced was the even-chain acetate obtained from EEO, which can be elongated to butyrate and then C6. Moreover, chain elongation to produce C7 has an intrinsic lower selectivity, since according to Eq.1, the production of 5 mol of C7 results in 1 mol of acetate, which is then elongated to C6. This has been experimentally proven by Grootscholten et al. (2013) and Roghair et al. (2018), who performed chain elongation on pure ethanol and propionate. In light of this, fermentation of wine lees as sole substrate would target C6, while the addition of WAS would give a mixture of C6 and C7 (Grootscholten et al., 2013; Kucek et al., 2016b). Co-fermentation could benefit the process compared to the use of wine lees as a sole substrate by buffering the pH, balancing the C/N ratio, and reducing water consumption for dilution, while providing the simultaneous treatment of two waste streams. After separation, the C6 and C7 mixture can be used for a variety of applications, such as jet fuel, biolubricants and biopolymers

production (Ho et al., 2019; Huq et al., 2021; Montiel-Corona and Buitrón, 2023) and additives in animal feed for pigs and poultry (Jackman et al., 2020; Szabó et al., 2023). C6 and C7 are also used in the pharmaceutical industry as antimicrobials and food supplements (Roopashree et al., 2021; Xu et al., 2024) and as flavor additives in the food industry (Junaid et al., 2023), although a high purity would be necessary for these applications, if authorized. The remaining carboxylates after MCCAs extraction, mainly constituted by acetate, could then be used as a substrate for subsequent biorefinery processes such as microalgae cultivation and microbial electrolysis cells.

3.2. Thermodynamic analysis

To better describe the metabolic routes that may occur in the system, the results of the thermodynamic analysis are reported in Table 2. At the beginning of the experiments, H_2 was not detected in the bottles, thus pH_2 was estimated from the equation of decomposition of water in O_2 and H_2 at equilibrium. This results in low values of ΔG of EEO and ethanol-based chain elongation at day 0.

On day 1, EEO was feasible in all conditions. In fact, ΔG values were below −20 kJ/mol, which is the generally accepted thermodynamic limit of microbial activity (Schink, 1997). This was due to the high ethanol concentration (85.1–455.7 mM) and low pH_2 ($4.01 \cdot 10^{-4}$-$1.25 \cdot 10^{-2}$ bar) detected in our bottles. However, ΔG became closer to the thermodynamic limit of −20 kJ/mol as the substrate (ethanol) concentration decreased and the products (acetate and H_2) concentration increased over time, with ΔG values ranging from –23.0 to −13.3 kJ/mol on day 3 (Table 2). Conversely, ethanol-based chain elongation was always thermodynamically favorable, with ΔG (kJ/mol) at day 1 ranging from −240.3 to −235.4 for C2→C4, from −261.5 to −213.4 for C4→C6, from −236.8 to −218.5 for C3→C5, and from −226.0 to −194.4 for C5→C7. ΔG values decreased over time due to substrate consumption and product formation, with a final value (kJ/mol) ranging from −219.1 to −189.2 for C2→C4, from −200.9 to −169.8 for C4→C6, from −151.2 to −184.2 for C3→C5, and from −219.8 to −199.9 for C5→C7. The carboxylates production and ethanol consumption dynamics presented in section 3.1 can be interpreted in light of these results. First, ethanol consumption and acetate production observed during the first 3 days were attributed to EEO. On day 3, acetate production almost stopped, consistently with the progressive increase of the ΔG of EEO. At 100 gCOD/L, it continued until day 4, even if with a slightly unfavorable ΔG of −16.2/-17.9 kJ/mol. This could be explained by heterogeneities in the bottle, with places where local pH_2 and ΔG values would have been lower than on a macroscopic scale. From a thermodynamic point of view, chain elongation could occur from day 1. However, as discussed in section 3.1, the occurrence of chain elongation depended also on the activity of specific chain-elongating microorganisms, which usually have a lag phase of several days (San-Valero et al., 2019). In this study, chain elongation started on day 2 with butyrate and valerate production and on day 3 with MCCAs production. MCCAs production started independently from butyrate and valerate concentrations, with a lag phase reasonably attributable to the time

Table 2
Daily values of the variation in Gibbs free energy of reaction (ΔG) for excessive ethanol oxidation (EEO) and ethanol-based chain elongation of C4 → C6 and C5 → C7. *= values calculated using pH_2 estimated from water decomposition at the equilibrium; green = thermodynamically feasible (ΔG < -20 kJ/mol); red = thermodynamically unfeasible (ΔG > -20 kJ/mol).

Condition	Day 0	Day 1	Day 2	Day 3	Day 4	Day 7	Day 0	Day 1	Day 2	Day 3	Day 4	Day 7
	ΔG excessive ethanol oxidation (EEO) kJ/mol											
20 gCOD/L	-451.5*	-32.4	-28.9	-18.6	-16.7							
40 gCOD/L	-451.8*	-29.5	-26.6	-23.0	-18.9							
70 gCOD/L	-451.2*	-25	-20.7	-13.3	-13.5							
100 gCOD/L	-453.7*	-22.2	-16.2	-17.9	-16.7	-19.1						
	ΔG chain elongation C2→C4 kJ/mol						**ΔG chain elongation C4→C6 kJ/mol**					
20 gCOD/L	-631.2*	-235.4	-223.7	-210.7	-189.2		-617.3*	-213.4	-254.3	-201.6	-169.8	
40 gCOD/L	-650.7*	-240.3	-227.2	-222.5	-196		-627.1*	-229.1	-246.9	-192.3	-178.2	
70 gCOD/L	-665.1*	-238.9	-225.1	-213.9	-219.1		-633.1*	-252.2	-255.8	-213.5	-182.1	
100 gCOD/L	-664.2*	-238.4	-226.5	-219.8	-218.6	-225.7	-640.4*	-261.5	-256.9	-267.1	-230.8	-200.9
	ΔG chain elongation C3→C5 kJ/mol						**ΔG chain elongation C5→C7 kJ/mol**					
20 gCOD/L	-642.8*	-221.8	-174.6	-175.4	-151.2		-620.9*	-199.9	-197	-167.9	-173.6	
40 gCOD/L	-652.6*	-228.1	-220.8	-171	-157.4		-630.7*	-206.3	-204.1	-240.5	-170.8	
70 gCOD/L	-658.6*	-236.8	-211.6	-176.7	-163.6		-636.7*	-203.8	-216.9	-234	-190.9	
100 gCOD/L	-665.9*	-218.5	-203	-195.5	-183.5	-166	-644*	-226	-227.3	-235.9	-244.7	-219.8

required for biomass to grow and adapt to the initial conditions (Steinbusch et al., 2011). Overall, the thermodynamic analysis showed that pH_2 was the main factor controlling EEO feasibility, while the increase in substrate concentration did not affect substantially the ΔG values. This finding provides some clues for controlling the chain elongation process. For instance, after converting the desired amount of ethanol to acetate, EEO could be stopped by injecting H_2 in the reactor to keep the minimum pH_2 required of 10^{-1} bar, thus steering the ethanol consumption pathway to chain elongation and therefore boosting MCCAs selectivities (Angenent and Agler, 2017). The thermodynamic analysis also showed that the differences observed at different substrate concentrations were not due to thermodynamic reasons, but rather to growth kinetics and inhibition from ethanol.

Lactate-based chain elongation was also always feasible, with values ranging from −68.3 to −56.1 for C2→C4, from −77.4 to −53.0 for C4→C6, from −67.9 to −50.9 for C3→C5, and from −71.6 to −53.6 for C5→C7 (Table S2).

3.3. Mass balance

Mass balances were conducted to understand the metabolic pathways involved in chain elongation and acetate production, considering i) only ethanol (Table 3A) or ii) only lactate (Table 3B) as electron donor in chain elongation. Butyrate and valerate were considered to be generated by chain elongation of acetate and propionate, respectively, and the fraction of acetate that was not produced through EEO or ethanol-based chain elongation was considered to be produced by the primary fermentation of the substrates, since low P_{H2} (<0.02 bar) and high acetate concentration (>10 mM) probably limited homoacetogenesis to a minimum (Bastidas-Oyanedel et al., 2012). In lactate-based chain elongation, all the ethanol consumption was attributed to EEO.

Table 3
Mass balance of ethanol and acetate in the different conditions tested to quantify ethanol consumption and acetate production and consumption in the metabolic reactions. The mass balance is relative to the whole duration of the experiment, i.e., day 7 at 100 gCOD/L and day 4 for the other conditions. *= net acetate produced, after removing the acetate used in biomass and HCO_3^- production.

A	Unit	20	40	70	100
		gCOD/L			
EtOH consumed (overall)	mMol C	17.9	35.6	31.3	35.6
EtOH consumed in chain elongation	**%**	**27.0**	**45.4**	**36.3**	**45.8**
C2→C4	%	12.4	13.6	13.2	19.7
C4→C6	%	8.0	11.4	12.4	13.6
C3→C5	%	4.0	3.1	5.2	9.7
C5→C7	%	2.6	17.4	5.4	2.8
EtOH consumed in EEO	**%**	**73.0**	**54.6**	**63.7**	**54.2**
Acetate produced in the test (measured)	mMol C	10.4	15.4	20.7	27.8
Acetate produced from EEO	**%**	**93.7**	**94.4**	**72.6**	**52.3**
Acetate produced from chain elongation*		**4.7**	**10.7**	**5.4**	**5.7**
Acetate produced from the substrates		**1.6**	**–**	**22.0**	**42.0**
Error in the mass balance	**%**	**0.0**	**−5.1**	**0.0**	**0.0**

B	Unit	20 gCOD/L	40	70	100
EtOH consumed (overall)	mMol C	17.9	35.6	31.3	35.6
EtOH consumed in EEO	**%**	**100.0**			
Lactate used in chain elongation	mMol C	3.7	9.3	9.3	12.4
Acetate produced in the test (measured)	mMol C	10.4	15.4	20.7	27.8
Acetate produced from EEO	**mMol C**	**13.4**	**26.7**	**23.6**	**26.8**
Acetate produced from the substrates		**–**	**–**	**–**	**1.0**
Error in the mass balance	**%**	**28.5**	**73.0**	**13.9**	**0.0**
CO_2 produced in the test					
Measured	mMol C	**0.5**	**1.1**	**4.5**	**4.5**
Calculated		**2.1**	**5.4**	**5.4**	**7.2**
Error in the mass balance	%	**346.7**	**376.2**	**20.7**	**60.5**

Considering an ethanol-based chain elongation, 27.0 to 45.8 % of the ethanol initially present in the substrates was used for chain elongation, while the remainder was consumed in EEO (Table 3A). The percentage of ethanol consumed converted *via* chain elongation was higher at 100 gCOD/L (45.8 %) respect to the other conditions (27.0–36.3 %). However, the overall ethanol consumption at day 7 (19.8 %) was lower than at 40 gCOD/L (67.1 %), where the highest C6 and C7 conversion and selectivities were obtained (Table 1). With the increase in substrate concentration, the percentage of acetate produced from the substrates increased. EEO was the main responsible for acetate production at 20 and 40 gCOD/L (93.7 and ~94.4 %, respectively), while at 70 and 100 gCOD/L a higher percentage of acetate was produced by fermentation of the substrates (22.0 and 42.0 %, respectively). With the assumption that the acetate not generated through EEO or chain elongation was obtained from the substrates, mass balances were closed with an error < 10 %. This was observed only at 40 gCOD/L, and it can be partially justified by the consumption of some acetate in the CH_4 production occurring at the end of the test.

Considering a lactate-based chain elongation, the acetate produced through EEO exceeded the acetate measured experimentally by 28.5, 73.0 and 13.9 % at 20, 40 and 70 gCOD/L, respectively, while it respected the mass balance at 100 gCOD/L. The CO_2 calculated from lactate-based chain elongation was considerably higher than the CO_2 measured experimentally at 20 and 40 gCOD/L (346.7–376.2 %), with a lower difference at 70 and 100 gCOD/L (20.7–60.5 %) which could be partially due to CO_2 consumption for biomass growth (Tomlinson and Barker, 1954).

In light of these results, chain elongation probably occurred using both ethanol and lactate as electron donors, with ethanol prevailing at 20 and 40 gCOD/L, and lactate at 70 and 100 gCOD/L. This supported the experimental observations of rapid chain elongation and high MCCAs selectivity, since ethanol- and lactate-based chain elongation seem to boost one each other. In fact, the CO_2 produced in the lactate-based pathway could have compensated for the CO_2 shortage in the ethanol-based one, necessary for the growth of chain-elongating microorganisms (Wu et al., 2018). The metabolic shift observed at 70 and 100 gCOD/L was underpinned by the cease in ethanol consumption with the beginning of chain elongation, alongside the detection of lactate (0.46 ± 0.04 g/L) at 100 gCOD/L on day 2 (Fig. 1). This supported a first oxidation of ethanol to acetate and lactate-based chain elongation.

3.4. Microbial communities

The analysis of microbial communities was conducted by sequencing of V3-V4 region of the 16S rRNA gene in samples from the fermentations at day 4 for all fermentations and in an additional sample at day 7 for the fermentation at 100 gCOD/L. From all these samples 897 OTUs were identified, which were grouped into 24 phyla, 46 classes, 96 orders, 187 families, and 361 genera. After filtering at 1 % of relative abundance, only 4 orders remained: *Bacteroidales*, *Eubacteriales* (formerly *Clostridiales*), *Enterobacteriales*, and *Lactobacillales*. Among them, only seven families had a relative abundance higher than 1 %: *Bacteroidaceae, Enterobacteriaceae, Enterococcaceae, Lachnospiraceae, Peptostreptococcaceae, Porphyromonadaceae,* and *Oscillospiraceae* (Table 4 and Supplementary Material). The rarefaction curves of all samples confirm that the sequencing depth was adequate for detecting the major components of the microbial diversity (Supplementary Material). Similar values were observed for richness. Shannon and Simpson diversity and

Table 4
Summary table of the microbial community analysis, reporting ecological indices and taxonomic composition of the fermented effluents at day 4 and at the end of the experiment (day 7 at 100 gCOD/L). Only taxa with a relative abundance ≥ 1 % were reported.

Ecological diversity	Closest species match	20 gCOD/L	40 gCOD/L	70 gCOD/L	100 gCOD/L	100_day7 gCOD/L
Richness		410	443	478	487	481
Shannon diversity		2.493	2.781	3.236	3.309	3.410
Simpson diversity		0.282	0.242	0.100	0.097	0.112
Pielou's evenness		0.414	0.456	0.525	0.535	0.541
Order, family and species		%				
BACTEROIDALES		**60.19**	**54.04**	**38.92**	**23.90**	**15.88**
Bacteroidaceae						
OTU 17	*Bacteroides faecis* (98.81 %)	8.69	5.89	15.37	12.4	6.22
Porphyromonadaceae						
OTU 3	*Macellibacteroides fermentans* (98.81 %)	51.50	48.15	23.55	11.50	9.66
ENTEROBACTERIALES		**12.4**	**7.84**	**9.79**	**8.12**	**6.94**
Enterobacteriaceae						
OTU 1	*Escherichia-Shigella* (100 %)	2.91	5.48	8.76	7.89	6.70
OTU 2	*Klebsiella pneumoniae* (98.59 %)	9.49	2.36	1.03	0.23	0.24
EUBACTERIALES		**8.06**	**12.73**	**24.28**	**28.69**	**32.85**
Clostridiaceae						
OTU 89	*Clostridium muellerianum* (94.76 %)	1.59	2.77	0.08	0.02	0.01
Lachnospiraceae						
OTU 11	*Roseburia intestinalis* (96.03 %)	1.32	2.02	13.90	22.02	27.34
Oscillospiraceae						
OTU 22	*Anaerofilum pentosovorans* (93.05 %) *Ruminiclostridium herbifermentans* (89.11 %)	3.51	3.39	6.38	3.60	2.71
OTU 69		0.43	2.68	1.97	0.50	0.72
Peptostreptococcaceae						
OTU 5	*Paraclostridium bifermentans* (97.25 %)	1.21	1.87	1.95	2.55	2.07
LACTOBACILLALES		**0.47**	**2.91**	**5.82**	**13.75**	**13.18**
Enterococcaceae						
OTU 6	*Enterococcus hirae* (99.53 %)	0.47	2.91	5.82	13.75	13.18

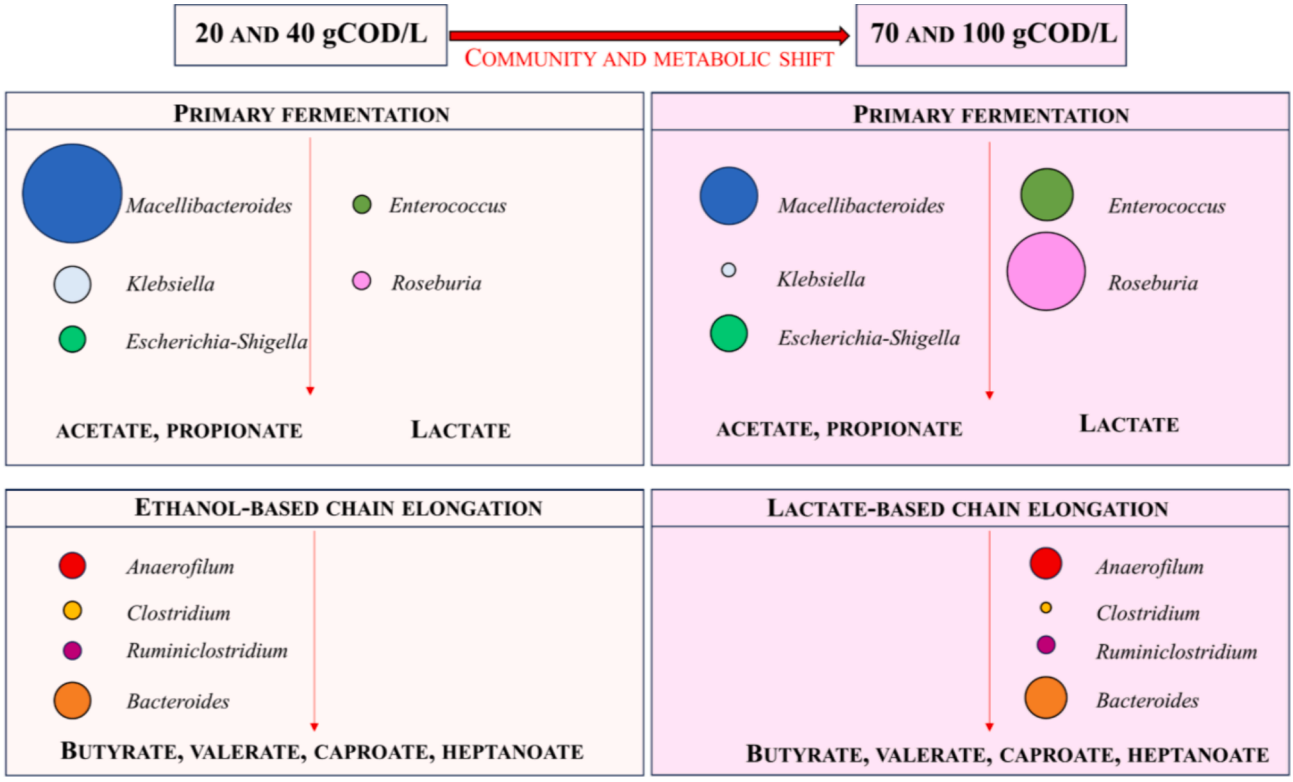

Fig. 2. Structure of the microbiome at 20 and 40 gCOD/L and 70 and 100 gCOD/L. A community shift is underlined, coherently with the metabolic shift from an ethanol- to a lactate-based chain elongation. The shift is marked by the genera *Macellibacteroides*, *Roseburia*, *Enterococcus*, and *Escherichia-Shigella*. The circles give an indication of the relative abundance of each genus, but the dimensions do not vary proportionally. See Table 4 for the exact relative abundances.

Pielou's evenness showed an increasing trend from 20 to 100 gCOD/L, since more species had a similar relative abundance (Table 4). Richness (410–481 OTUs) was lower than WAS (820) and higher than wine lees (60), indicating that a selection occurred and that the WAS microbiome mainly shaped the fermentative community. Richness was lower than other biological processes, i.e., anaerobic digestion (~1000 OTUs) (Pasalari et al., 2021). The community was dominated by few species (Shannon Index 2.5–3.4), many of which represented a similar proportion of the community, as indicated by the average value of Pielou's evenness (0.414–0.541). Diversity was comparable to reported observations with continuous fermentation of wine lees for C6 and C8 production using synthetic ethanol and lactate as electron donors (Shannon Index 3.4–3.7) (Kucek et al., 2016a; 2016b). This indicates that the lower yields observed at 70 and 100 gCOD/L were not due to a decrease in microbial diversity, as suggested elsewhere (Wu et al., 2016; Zhang et al., 2020a). Coherently, PCoA showed a consistent evolution of the microbial community from aerobic (substrates) to anaerobic (after fermentation), with no clustering based on substrate concentration (Supplementary Material).

Respect to the microbial community composition, a chain-elongating microbiome was developed, allowing for the fast chain elongation described in the previous sections. The community was dominated by the *Bacteroidales* (15.9–60.2 %) and *Eubacteriales* (8.06–32.9 %) orders, both widely reported to be positively correlated with MCCAs production using ethanol as electron donor (Table 4) (Kucek et al., 2016b; Wu et al., 2020). However, the chain elongation ability in these orders is highly variable, depending on families and genera and has started being explored only in the last 10 years, as reviewed by Candry and Ganigué (2021). At the family level, the community was enriched in *Lachnospiraceae* (1.3–27.3 %), *Clostridiaceae* (0.01–2.8 %), and *Oscillospiraceae* (3.4–8.4 %) to which several chain-elongating genera belong (Table 4) (Candry and Ganigué, 2021 and references therein). Among the OTUs identifiable as chain-elongating species, only *Clostridium muellerianum* (OTU 89, 94.8 % identity) was already described to produce C6, while the ability to perform chain elongation can be hypothesized for the members of the *Oscillospiraceae* family, into which four of the most recently identified chain elongators have been placed (Esquivel-Elizondo et al., 2021; Liu et al., 2020). Our community was also enriched in the putative chain-elongator *Bacteroides* (5.9–15.4 %), reported to be positively correlated with MCCAs productivity (Kucek et al., 2016b). However, no correlation was observed in the present study. This does not exclude that *Bacteroides* spp. have chain elongation abilities, but these should be confirmed with physiological studies, since functions cannot be unequivocally inferred from correlations.

As summarized in Fig. 2, a shift in the microbial community composition was observed from 20 and 40 gCOD/L to 70 and 100 gCOD/L, consistently with the metabolic shift from an ethanol-based to a probable lactate-based chain elongation. The main markers of this shift were members of the *Porphyromonadaceae* (OTU 3), *Lachnospiraceae* (OTU 11), *Enterococcaceae* (OTU 6), and *Enterobacteriaceae* (OTU 1) family, identified as the hydrolytic and acidogenic genera *Macellibacteroides*, *Roseburia*, *Enterococcus*, and *Escherichia-Shigella,* respectively. *Macellibacteroides* was dominant at the lowest substrate concentrations, ranging from 51.5 % at 20 gCOD/L to 23.6 % at 70 gCOD/L (Table 4). At 70 gCOD/L, *Roseburia* started to increase its relative abundance (13.9 %), becoming prevalent at 100 gCOD/L (22.0–27.3 %), where *Macellibacteroides* dropped to 9.7–11.5 %. *Enterococcus* abundances increased at increasing substrate concentrations, representing 0.5, 3.0, 5.8, and 13.8 % of the community at 20, 40, 70, and 100 gCOD/L on day 4, respectively. Finally, the relative abundance of *Escherichia-Shigella* increased with substrate concentration, representing 8.8–7.9 % of the community on day 4 at 70 and 100 gCOD/L, respectively. OTU 3 of the *Porphyromonadaceae* family had 98.8 % similarity with *Macellibacteroides fermentans*, a mesophilic, fermentative, and obligately anaerobic genus firstly isolated from an upflow anaerobic filter treating abattoir wastewaters with lactate, acetate, butyrate and *iso*-butyrate as the main fermentation products from glucose metabolism (Jabari et al., 2012). The fermentation studies found in literature confirm the acidogenic role of *Macellibacteroides*, that was enriched in WAS fermentation after substrate pretreatment and in a chain-elongating microbiome, where it was considered a butyrate producer (She et al., 2020; Xiang et al., 2023; Xie et al., 2022). OTU 11 (class *Clostridia*, order *Eubacteriales*, family *Lachnospiraceae*) had 96.0 % similarity with *Roseburia intestinalis*, an anaerobic species with butyrate and L-lactate identified as the major products, and able to use acetate to improve its growth (Duncan et al., 2002). Its identification in fermentation studies is limited and considered *Roseburia* to be a lactate and butyrate producer in chain-elongating microbiomes (Scarborough et al., 2018). It cannot be excluded that *Roseburia* and *Macellibacteroides* can also perform chain elongation, even though their presence in chain-elongating microbiomes was rare and mainly related to butyrate production (Scarborough et al., 2018; Xiang et al., 2023). In light of the metabolic shift to lactate-based chain elongation observed at 70 and 100 gCOD/L, in correspondence to the increase in the relative abundance of *Roseburia*, it can be hypothesized that this genus was mainly a lactate producer, while *Macellibacteroides* was mainly a SCFAs producer. Alongside *Roseburia*, also the increase in the relative abundance of *Enterococcus* at 70 and 100 gCOD/L supported the hypothesis of a metabolic shift to lactate-based chain elongation, with lactate produced and immediately consumed as electron donor. In fact OTU 6, belonging to the *Enterococcaceae* family, had 99.53 % similarity with *Enterococcus hirae*, a facultative anaerobic, L-lactic acid producing bacteria (Farrow and Collins, 1985). Finally, OTU 1 of the *Enterobacteriaceae* family had 100 % similarity with *Escherichia-Shigella* genus, composed by hydrolytic, SCFAs-producing microorganisms widely observed in liquor fermentation systems, and were recently reported to increase their abundance at high ethanol concentrations (0–170 mM) in the fermentation of WAS with ethanol addition (Dai et al., 2019; Wu et al., 2021). Therefore, the observed increase in *Escherichia-Shigella* was attributable to the higher ethanol concentrations and longer time needed to hydrolyze high concentrations of substrates.

Finally, while the hydrolytic, acidogenic and chain-elongating activity in our microbiome could be attributed to specific genera as discussed above, the same was not possible for EEO. At present, EEO is known to be conducted by sulfate-reducing bacteria in absence of sulfate, such as *Desulfovibrio* spp. (Plugge et al., 2011; Roghair et al., 2018), and by *Acetobacterium woodii* (Bertsch et al., 2016), which were absent in our community. However, EEO-related genes were found in *Clostridium* spp., which could have contributed to this reaction also in our microbiome (Tao et al., 2017; Wu et al., 2020).

4. Conclusions

Wine lees and WAS were successfully co-fermented and upgraded to C6 and C7 with the highest selectivity of 40.2 % at 40 gCOD/L, thanks to a rapidly-growing chain-elongating microbiome led by *Clostridium muellerianum, Anaerofilum pentosovorans*, and *Ruminiclostridium herbifermentans*, representing together 3.4–8.8 % of the community. The C7 selectivity obtained (16 % on COD basis) is the highest observed at pH 7.0 on complex substrates without external ethanol supplementation. Both C6 and C7 selectivities could be improved in a continuous reactor, where the process sustainability should be confirmed. Thermodynamic analysis identified pH_2 as the fundamental parameter to control ethanol conversion to acetate, thereby maximizing MCCAs selectivities.

CRediT authorship contribution statement

A. Lanfranchi: Writing – review & editing, Writing – original draft, Visualization, Investigation, Formal analysis, Data curation, Conceptualization. **E. Desmond-Le Quéméner:** Formal analysis, Writing – review & editing. **J.A. Magdalena:** Writing – review & editing, Supervision. **C. Cavinato:** Supervision, Funding acquisition, Conceptualization. **E.**

Trably: Writing – review & editing, Supervision, Resources, Funding acquisition, Conceptualization.

Declaration of competing interest

The authors declare that they have no known competing financial interests or personal relationships that could have appeared to influence the work reported in this paper.

Data availability

Sequences are available in GenBank, under the accession number PRJNA1028514. Data will be made available upon request.

Acknowledgments

Alice Lanfranchi would like to thank the Italian Ministry of Education and Merit for funding her PhD scholarship. Jose Antonio Magdalena would like to thank the Complutense University of Madrid for the financing of his contract at LBE-INRAE (France), with funds from the Ministry of Universities for the requalification of the Spanish University System for 2021–2023 (Modality 1. Margarita Salas), coming from the European Union-Next generation EU funding. This work was partially supported by DAIS- Ca' Foscari University of Venice within the IRIDE program. Analyses and experiments were performed at the Bio2E platform (doi:10.5454/1.557234103446854E12).

Appendix A. Supplementary data

Supplementary data to this article can be found online at https://doi.org/10.1016/j.biortech.2024.131126.

References

Agler, M.T., Spirito, C.M., Usack, J.G., Werner, J.J., Angenent, L.T., 2014. Development of a highly specific and productive process for n-caproic acid production: applying lessons from methanogenic microbiomes. Water Sci. Technol. 69, 62–68. https://doi.org/10.2166/wst.2013.549.

Angenent, L.T., Agler, M.T., 2017. Production of carboxylates and methane from biomass waste. US 9650652, B2.

Barker, H.A., 1947. Clostridium kluyveri. Antonie Van Leeuwenhoek 12, 167–176.

Bastidas-Oyanedel, J.R., Mohd-Zaki, Z., Zeng, R.J., Bernet, N., Pratt, S., Steyer, J.P., Batstone, D.J., 2012. Gas controlled hydrogen fermentation. Bioresour Technol 110, 503–509. https://doi.org/10.1016/j.biortech.2012.01.122.

Bertsch, J., Siemund, A.L., Kremp, F., Müller, V., 2016. A novel route for ethanol oxidation in the acetogenic bacterium Acetobacterium woodii: the acetaldehyde/ethanol dehydrogenase pathway. Environ Microbiol 18, 2913–2922. https://doi.org/10.1111/1462-2920.13082.

Bevilacqua, R., Regueira, A., Mauricio-Iglesias, M., Lema, J.M., Carballa, M., 2022. Chain elongation may occur in protein mixed-culture fermentation without supplementing electron donor compounds. J Environ Chem Eng 10, 106943. https://doi.org/10.1016/J.JECE.2021.106943.

Candry, P., Ganigué, R., 2021. Chain elongators, friends, and foes. Curr Opin Biotechnol 67, 99–110. https://doi.org/10.1016/j.copbio.2021.01.005.

Carvajal-Arroyo, J.M., Andersen, S.J., Ganigué, R., Rozendal, R.A., Angenent, L.T., Rabaey, K., 2021. Production and extraction of medium chain carboxylic acids at a semi-pilot scale. Chem. Eng. J. 416 https://doi.org/10.1016/j.cej.2020.127886.

Chen, W.S., Strik, D.P.B.T.B., Buisman, C.J.N., Kroeze, C., 2017. Production of caproic acid from mixed organic waste: an environmental life cycle perspective. Environ Sci Technol 51, 7159–7168. https://doi.org/10.1021/acs.est.6b06220.

European Commission, 2019. COMMUNICATION FROM THE COMMISSION TO THE EUROPEAN PARLIAMENT. THE EUROPEAN COUNCIL, THE COUNCIL. THE EUROPEAN ECONOMIC AND SOCIAL COMMITTEE AND THE COMMITTEE OF THE REGIONS The European Green Deal COM/2019/640 final.

Da Ros, C., Cavinato, C., Pavan, P., Bolzonella, D., 2017. Mesophilic and thermophilic anaerobic co-digestion of winery wastewater sludge and wine lees: an integrated approach for sustainable wine production. J Environ Manage 203, 745–752. https://doi.org/10.1016/j.jenvman.2016.03.029.

Dai, Y., Tian, Z., Meng, W., Li, C., Li, Z., 2019. Changes in microbial diversity, physicochemical characteristics, and flavor substances during maotai-flavored liquor fermentation and their correlations. J Biobased Mater Bioenergy 13, 290–307. https://doi.org/10.1166/jbmb.2019.1866.

Das, G., Trivedi, R.K., Vasishtha, A.K., 1989. Heptaldehyde and undecylenic acid from castor oil. J Am Oil Chem Soc 66, 938–941. https://doi.org/10.1007/BF02682613.

Debergh, P., Van Dael, M., 2022. Production of caproic acid from acetate and ethanol through microbial chain elongation: a techno-economic assessment. Bioresour Technol Rep 18, 101055. https://doi.org/10.1016/J.BITEB.2022.101055.

Duncan, S.H., Hold, G.L., Barcenilla, A., Stewart, C.S., Flint, H.J., 2002. Roseburia intestinalis sp. nov., a novel saccharolytic, butyrate-producing bacterium from human faeces. Int J Syst Evol Microbiol 52, 1615–1620. https://doi.org/10.1099/ijs.0.02143-0.

Esquivel-Elizondo, S., Bağcı, C., Temovska, M., Jeon, B.S., Bessarab, I., Williams, R.B.H., Huson, D.H., Angenent, L.T., 2021. The Isolate Caproiciproducens sp. 7D4C2 Produces n-Caproate at Mildly Acidic Conditions From Hexoses: Genome and rBOX Comparison With Related Strains and Chain-Elongating Bacteria. Front Microbiol 11. https://doi.org/10.3389/fmicb.2020.594524.

Esteban-Gutiérrez, M., Garcia-Aguirre, J., Irizar, I., Aymerich, E., 2018. From sewage sludge and agri-food waste to VFA: Individual acid production potential and up-scaling. Waste Manage 77, 203–212. https://doi.org/10.1016/J.WASMAN.2018.05.027.

Farrow, J.A.E., Collins, M.D., 1985. Enterococcus hirae, a new species that includes amino acid assay strain NCDO 1258 and strains causing growth depression in young chickens. Int J Syst Bacteriol 35, 73–75. https://doi.org/10.1099/00207713-35-1-73.

Ge, S., Usack, J.G., Spirito, C.M., Angenent, L.T., 2015. Long-term n-caproic acid production from yeast-fermentation beer in an anaerobic bioreactor with continuous product extraction. Environ Sci Technol 49, 8012–8021. https://doi.org/10.1021/acs.est.5b00238.

Grootscholten, T.I.M., Steinbusch, K.J.J., Hamelers, H.V.M., Buisman, C.J.N., 2013. High rate heptanoate production from propionate and ethanol using chain elongation. Bioresour Technol 136, 715–718. https://doi.org/10.1016/J.BIORTECH.2013.02.085.

Ho, C.K., McAuley, K.B., Peppley, B.A., 2019. Biolubricants through renewable hydrocarbons: a perspective for new opportunities. Renew. Sustain. Energy Rev. https://doi.org/10.1016/j.rser.2019.109261.

Huq, N.A., Hafenstine, G.R., Huo, X., Nguyen, H., Tifft, S.M., Conklin, D.R., Stück, D., Stunkel, J., Yang, Z., Heyne, J.S., Wiatrowski, M.R., Zhang, Y., Tao, L., Zhu, J., Mcenally C , C.S., Christensen, E.D., Hays, C., Van Allsburg, K.M., Unocic, K.A., Iii, H.M.M., Abdullah, Z., Vardon, D.R., 2021. Toward net-zero sustainable aviation fuel with wet waste-derived volatile fatty acids. Proceedings of the National Academy of Sciences 118. https://doi.org/10.1073/pnas.2023008118/-/DCSupplemental.

Jabari, L., Gannoun, H., Cayol, J.L., Hedi, A., Sakamoto, M., Falsen, E., Ohkuma, M., Hamdi, M., Fauque, G., Ollivier, B., Fardeau, M.L., 2012. Macellibacteroides fermentans gen. nov., sp. nov., a member of the family Porphyromonadaceae isolated from an upflow anaerobic filter treating abattoir wastewaters. Int J Syst Evol Microbiol 62, 2522–2527. https://doi.org/10.1099/ijs.0.032508-0.

Jackman, J.A., Boyd, R.D., Elrod, C.C., 2020. Medium-chain fatty acids and monoglycerides as feed additives for pig production: towards gut health improvement and feed pathogen mitigation. J Anim Sci Biotechnol 11. https://doi.org/10.1186/s40104-020-00446-1.

Junaid, M., Inayat, S., Gulzar, N., Khalique, A., Shahzad, F., Irshad, I., Imran, M., 2023. Physical, chemical, microbial, and sensory evaluation and fatty acid profiling of value-added drinking yogurt (laban) under various storage conditions. J Dairy Sci 106, 39–46. https://doi.org/10.3168/jds.2022-22358.

Kim, B.C., Moon, C., Jeon, B.S., Angenent, L.T., Choi, Y., Nam, K., 2021. Shaping a reactor microbiome generating stable n-caproate productivity through Design-Build-Test-Learn approach. Chem. Eng. J. 425 https://doi.org/10.1016/j.cej.2021.131587.

Kleerebezem, R., Van Loosdrecht, M.C.M., 2010. A generalized method for thermodynamic state analysis of environmental systems. Crit Rev Environ Sci Technol 40, 1–54. https://doi.org/10.1080/10643380802000974.

Kucek, L.A., Nguyen, M., Angenent, L.T., 2016a. Conversion of l-lactate into n-caproate by a continuously fed reactor microbiome. Water Res 93, 163–171. https://doi.org/10.1016/J.WATRES.2016.02.018.

Kucek, L.A., Xu, J., Nguyen, M., Angenent, L.T., 2016b. Waste conversion into n-caprylate and n-caproate: resource recovery from wine lees using anaerobic reactor microbiomes and in-line extraction. Front Microbiol 7. https://doi.org/10.3389/fmicb.2016.01892.

Lesteur, M., Latrille, E., Maurel, V.B., Roger, J.M., Gonzalez, C., Junqua, G., Steyer, J.P., 2011. First step towards a fast analytical method for the determination of Biochemical Methane Potential of solid wastes by near infrared spectroscopy. Bioresour Technol 102, 2280–2288. https://doi.org/10.1016/J.BIORTECH.2010.10.044.

Liu, Y., Chen, L., Duan, Y., Li, R., Yang, Z., Liu, S., Li, G., 2024. Recent progress and prospects for chain elongation of transforming biomass waste into medium-chain fatty acids. Chemosphere 355. https://doi.org/10.1016/j.chemosphere.2024.141823.

Liu, B., Popp, D., Sträuber, H., Harms, H., Kleinsteuber, S., 2020. Draft genome sequences of three clostridia isolates involved in lactate-based chain elongation. Microbiol Resour Announc 9. https://doi.org/10.1128/mra.00679-20.

Lonkar, S., Fu, Z., Holtzapple, M., 2016. Optimum alcohol concentration for chain elongation in mixed-culture fermentation of cellulosic substrate. Biotechnol Bioeng 113, 2597–2604. https://doi.org/10.1002/bit.26024.

Martinez, G.A., Puccio, S., Domingos, J.M.B., Morselli, E., Gioia, C., Marchese, P., Raspolli Galletti, A.M., Celli, A., Fava, F., Bertin, L., 2022. Upgrading grape pomace contained ethanol into hexanoic acid, fuel additives and a sticky polyhydroxyalkanoate: an effective alternative to ethanol distillation. Green Chem. 24, 2882–2892. https://doi.org/10.1039/d2gc00044j.

Montiel-Corona, V., Buitrón, G., 2023. Polyhydroxyalkanoates and 5-aminolevulinic acid production by a mixed phototrophic culture using medium-chain carboxylic acids

from winery effluents. Bioresour Technol 373. https://doi.org/10.1016/j.biortech.2023.128704.
Moscoviz, R., Trably, E., Bernet, N., Carrère, H., 2018. The environmental biorefinery: state-of-the-art on the production of hydrogen and value-added biomolecules in mixed-culture fermentation †. Green Chem. 20 https://doi.org/10.1039/c8gc00572a.
Noguer, M.C., Magdalena, J.A., Bernet, N., Escudié, R., Trably, E., 2022. Enhanced fermentative hydrogen production from food waste in continuous reactor after butyric acid treatment. Energies (basel) 15, 1–18. https://doi.org/10.3390/en15114048.
Pasalari, H., Gholami, M., Rezaee, A., Esrafili, A., Farzadkia, M., 2021. Perspectives on microbial community in anaerobic digestion with emphasis on environmental parameters: a systematic review. Chemosphere. https://doi.org/10.1016/j.chemosphere.2020.128618.
Platt, Richard., Bauen, Ausilio., Reumerman, Patrick., Geier, C., Van Ree, R., Vural Gursel, Iris., Garcia, Lesly., Behrens, Martin., Bothmer, P. von., Howes, Jo., Panchaksharam, Yamini., Vikla, Kaisa., Sartorius, Valerie., Annevelink, Bert., European Commission. Directorate-General for Research and Innovation., E4tech., WUR., BTG., FNR., ICONS., 2021. EU biorefinery outlook to 2030 : studies on support to research and innovation policy in the area of bio-based products and services. https://doi.org/10.2777/103465.
Plugge, C.M., Zhang, W., Scholten, J.C.M., Stams, A.J.M., 2011. Metabolic flexibility of sulfate-reducing bacteria. Front Microbiol 2, 1–8. https://doi.org/10.3389/fmicb.2011.00081.
Roghair, M., Hoogstad, T., Strik, D.P.B.T.B., Plugge, C.M., Timmers, P.H.A., Weusthuis, R.A., Bruins, M.E., Buisman, C.J.N., 2018. Controlling ethanol use in chain elongation by CO2 loading rate. Environ Sci Technol 52, 1496–1506. https://doi.org/10.1021/acs.est.7b04904.
Roopashree, P.G., Shetty, S.S., Suchetha Kumari, N., 2021. Effect of medium chain fatty acid in human health and disease. J Funct Foods. https://doi.org/10.1016/j.jff.2021.104724.
Roslan, E., Magdalena, J.A., Mohamed, H., Akhiar, A., Shamsuddin, A.H., Carrere, H., Trably, E., 2023. Lactic acid fermentation of food waste as storage method prior to biohydrogen production: effect of storage temperature on biohydrogen potential and microbial communities. Bioresour Technol 378, 128985. https://doi.org/10.1016/J.BIORTECH.2023.128985.
San-Valero, P., Fernández-Naveira, Veiga, M.C., Kennes, C., 2019. Influence of electron acceptors on hexanoic acid production by Clostridium kluyveri. J Environ Manage 242, 515–521. https://doi.org/10.1016/J.JENVMAN.2019.04.093.
Scarborough, M.J., Lynch, G., Dickson, M., McGee, M., Donohue, T.J., Noguera, D.R., 2018. Increasing the economic value of lignocellulosic stillage through medium-chain fatty acid production. Biotechnol Biofuels 11, 1–17. https://doi.org/10.1186/s13068-018-1193-x.
Schink, B., 1997. Energetics of syntrophic cooperation in methanogenic degradation. Microbiol. Mol. Biol. Rev. 61, 262–280. https://doi.org/10.1128/mmbr.61.2.262-280.1997.
Shahid, F., 2005. Volume 1, Edible Oils and Fat Products: Chemistry, Properties, and Health Effects, in: Bailey's Industrial Oil and Fat Products. John Wiley & Sons Inc., Hoboken, p. 629.
She, Y., Hong, J., Zhang, Q., Chen, B.Y., Wei, W., Xin, X., 2020. Revealing microbial mechanism associated with volatile fatty acids production in anaerobic acidogenesis of waste activated sludge enhanced by freezing/thawing pretreatment. Bioresour Technol 302, 122869. https://doi.org/10.1016/J.BIORTECH.2020.122869.
Springer, H., Lappe, P., 2001. Deutsche Patentschrift DE 10010771. Verfahren zur Herstellung aliphatischer Carbonsäuren aus Aldehyden.
Steinbusch, K.J.J., Hamelers, H.V.M., Plugge, C.M., Buisman, C.J.N., 2011. Biological formation of caproate and caprylate from acetate: Fuel and chemical production from low grade biomass. Energy Environ Sci 4, 216–224. https://doi.org/10.1039/c0ee00282h.
Szabó, R.T., Kovács-Weber, M., Zimborán, Á., Kovács, L., Erdélyi, M., 2023. Effects of short- and medium-chain fatty acids on production, meat quality, and microbial attributes—a review. Molecules. https://doi.org/10.3390/molecules28134956.
Tao, Y., Wang, X., Li, X., Wei, N., Jin, H., Xu, Z., Tang, Q., Zhu, X., 2017. The functional potential and active populations of the pit mud microbiome for the production of Chinese strong-flavour liquor. Microb Biotechnol 10, 1603–1615. https://doi.org/10.1111/1751-7915.12729.
Tomlinson, N., Barker, H.A., 1954. Carbon dioxide and acetate utilization by Clostridium kluyveri. II. Synthesis of amino acids. J Biol Chem 209, 585–595.
Turpeinen, A., Merimaa, P., 2011. Functional fats and spreads, Functional Foods: Concept to Product: Second Edition. Woodhead Publishing Limited. https://doi.org/10.1533/9780857092557.3.383.
Villegas-Rodríguez, S.B., Arreola-Vargas, J., Buitrón, G., 2024. Influence of pH and temperature on the performance and microbial community during the production of medium-chain carboxylic acids using winery effluents as substrate. Environ. Sci. Pollut. Res. https://doi.org/10.1007/s11356-024-33103-5.
Villegas-Rodríguez, S., Buitrón, G., 2021. Performance of native open cultures (winery effluents, ruminal fluid, anaerobic sludge and digestate) for medium-chain carboxylic acid production using ethanol and acetate. J. Water Process Eng. 40, 101784 https://doi.org/10.1016/J.JWPE.2020.101784.
Wallace, R.J., McKain, N., McEwan, N.R., Miyagawa, E., Chaudhary, L.C., King, T.P., Walker, N.D., Apajalahti, J.H.A., Newbold, C.J., 2003. Eubacterium pyruvativorans sp. nov., a novel non-saccharolytic anaerobe from the rumen that ferments pyruvate and amino acids, forms caproate and utilizes acetate and propionate. Int J Syst Evol Microbiol 53, 965–970. https://doi.org/10.1099/ijs.0.02110-0.
Wallace, R.J., Chaudhary, L.C., Miyagawa, E., McKain, N., Walker, N.D., 2004. Metabolic properties of Eubacterium pyruvativorans, a ruminal "hyper-ammonia-producing" anaerobe with metabolic properties analogous to those of Clostridium kluyveri. Microbiology (n y) 150, 2921–2930. https://doi.org/10.1099/mic.0.27190-0.
Weimer, P.J., Stevenson, D.M., 2012. Isolation, characterization, and quantification of Clostridium kluyveri from the bovine rumen. Appl Microbiol Biotechnol 94, 461–466. https://doi.org/10.1007/s00253-011-3751-z.
Wu, P., Ding, P., Cao, Q. hao, Zhang, C., Fu, B., Liu, Hong bo, Chen, C. jun, Liu, He, 2023. Amino acids as in-situ electron donors drive medium chain fatty acids production from sludge acidogenic fermentation liquid by electro-fermentation enhancement. Chem Eng J 476. https://doi.org/10.1016/j.cej.2023.146537.
Wu, Q.L., Guo, W.Q., Zheng, H.S., Luo, H.C., Feng, X.C., Yin, R.L., Ren, N.Q., 2016. Enhancement of volatile fatty acid production by co-fermentation of food waste and excess sludge without pH control: the mechanism and microbial community analyses. Bioresour Technol 216, 653–660. https://doi.org/10.1016/J.BIORTECH.2016.06.006.
Wu, Q., Guo, W., Bao, X., Meng, X., Yin, R., Du, J., Zheng, H., Feng, X., Luo, H., Ren, N., 2018. Upgrading liquor-making wastewater into medium chain fatty acid: insights into co-electron donors, key microflora, and energy harvest. Water Res 145, 650–659. https://doi.org/10.1016/j.watres.2018.08.046.
Wu, S.L., Sun, J., Chen, X., Wei, W., Song, L., Dai, X., Ni, B.J., 2020. Unveiling the mechanisms of medium-chain fatty acid production from waste activated sludge alkaline fermentation liquor through physiological, thermodynamic and metagenomic investigations. Water Res 169, 115218. https://doi.org/10.1016/j.watres.2019.115218.
Wu, S.L., Luo, G., Sun, J., Wei, W., Song, L., Ni, B.J., 2021. Medium chain fatty acids production from anaerobic fermentation of waste activated sludge. J Clean Prod 279, 123482. https://doi.org/10.1016/j.jclepro.2020.123482.
Xiang, S., Wu, Q., Ren, W., Guo, W., Ren, N., 2023. Mechanism of powdered activated carbon enhancing caproate production. Chin. Chem. Lett. 34, 107714 https://doi.org/10.1016/J.CCLET.2022.07.057.
Xie, J., Xin, X., Ai, X., Hong, J., Wen, Z., Li, W., Lv, S., 2022. Synergic role of ferrate and nitrite for triggering waste activated sludge solubilisation and acidogenic fermentation: Effectiveness evaluation and mechanism elucidation. Water Res 226 (1), 119287. https://doi.org/10.1016/j.watres.2022.119287.
Xu, J., Qiao, H., Gan, L., Wang, P., Wang, J., Cui, Y., Zhou, J., Liu, Q., Jiang, Y., Zhang, H., Yang, K., 2024. Zinc caproate: ecofriendly synthesis, structural characterization, and antibacterial action. Int J Pharm 655. https://doi.org/10.1016/j.ijpharm.2024.124030.
Zhang, L., Loh, K.C., Dai, Y., Tong, Y.W., 2020a. Acidogenic fermentation of food waste for production of volatile fatty acids: bacterial community analysis and semi-continuous operation. Waste Manag. 109, 75–84. https://doi.org/10.1016/J.WASMAN.2020.04.052.
Zhang, W., Yin, F., Dong, H., Cao, Q., Wang, S., Xu, J., Zhu, Z., 2020b. Bioconversion of swine manure into high-value products of medium chain fatty acids. Waste Manag. 113, 478–487. https://doi.org/10.1016/j.wasman.2020.06.021.